

Award Number:
W81XWH-08-1-0572

TITLE: RNAi as a Routine Route Toward Breast Cancer Therapy

PRINCIPAL INVESTIGATOR:
Gregory J. Hannon, Ph.D.

CONTRACTING ORGANIZATION:
Cold Spring Harbor Laboratory
Cold Spring Harbor, NY 11724

REPORT DATE:
September 2013

TYPE OF REPORT:
Annual

PREPARED FOR: U.S. Army Medical Research and Materiel Command
Fort Detrick, Maryland 21702-5012

DISTRIBUTION STATEMENT:

Approved for public release; distribution unlimited

The views, opinions and/or findings contained in this report are those of the author(s) and should not be construed as an official Department of the Army position, policy or decision unless so designated by other documentation.

REPORT DOCUMENTATION PAGE				Form Approved OMB No. 0704-0188	
Public reporting burden for this collection of information is estimated to average 1 hour per response, including the time for reviewing instructions, searching existing data sources, gathering and maintaining the data needed, and completing and reviewing this collection of information. Send comments regarding this burden estimate or any other aspect of this collection of information, including suggestions for reducing this burden to Department of Defense, Washington Headquarters Services, Directorate for Information Operations and Reports (0704-0188), 1215 Jefferson Davis Highway, Suite 1204, Arlington, VA 22202-4302. Respondents should be aware that notwithstanding any other provision of law, no person shall be subject to any penalty for failing to comply with a collection of information if it does not display a currently valid OMB control number. PLEASE DO NOT RETURN YOUR FORM TO THE ABOVE ADDRESS.					
1. REPORT DATE (DD-MM-YYYY) September 2013		2. REPORT TYPE Annual		3. DATES COVERED (From - To) 1 SEP 2012 - 31 AUG 2013	
4. TITLE AND SUBTITLE RNAi as a Routine Route Toward Breast Cancer Therapy				5a. CONTRACT NUMBER .	
				5b. GRANT NUMBER W81XWH - 08 - 1 - 0572	
				5c. PROGRAM ELEMENT NUMBER	
6. AUTHOR(S) Gregory J. Hannon, PhD. go chrj cppqpB euj rtf w				5d. PROJECT NUMBER	
				5e. TASK NUMBER	
				5f. WORK UNIT NUMBER	
7. PERFORMING ORGANIZATION NAME(S) AND ADDRESS(ES) Cold Spring Harbor Laboratory Cold Spring Harbor, NY 11724				8. PERFORMING ORGANIZATION REPORT NUMBER	
9. SPONSORING / MONITORING AGENCY NAME(S) AND ADDRESS(ES) US Army Medical Research and Materiel Command Fort Detrick, MA 21702				10. SPONSOR/MONITOR'S ACRONYM(S)	
				11. SPONSOR/MONITOR'S REPORT NUMBER(S)	
12. DISTRIBUTION / AVAILABILITY STATEMENT Approved for public release; distribution unlimited					
13. SUPPLEMENTARY NOTES					
14. ABSTRACT During the first year of this innovator award, we made significant progress toward two of our aims. We constructed a third generation RNAi library and made that available to the breast cancer community. This resource has nearly 75,000 independent, sequence verified clones targeting ~18,000 human genes. A similar library for the mouse genome is nearing completion. We also scaled up our shRNA screening platform in preparation for lethality surveys of all suitable and available BC cell lines, including matched pairs of lines that have acquired resistance to herceptin in vitro. Relevant to our second aim, we have profiled microRNA from each of the identifiable epithelial cell types in the mouse mammary gland and are undertaking similar efforts in human. The goal is to develop microRNA sensor strategies that will permit visualization of each cell type in vivo and enable their isolation and manipulation in vitro. Finally, we showed that two microRNAs, let-7 and miR-93, can deplete tumor initiating cells from a number of basal breast cancer cell lines.					
15. SUBJECT TERMS RNAi, sequencing					
16. SECURITY CLASSIFICATION OF:			17. LIMITATION OF ABSTRACT UU	18. NUMBER OF PAGES 20	19a. NAME OF RESPONSIBLE PERSON USAMRMC
a. REPORT U	b. ABSTRACT U	c. THIS PAGE U			19b. TELEPHONE NUMBER (include area code)

Table of Contents

	<u>Page</u>
Cover.....	1
SF298.....	2
Table of Contents.....	3
Introduction.....	4
Body.....	4
Reportable Outcomes.....	8
Conclusion.....	8
Appendix	9

INTRODUCTION

The goal of this innovator award is to continue to develop and apply RNAi-based screening methods to discover new paths towards breast cancer treatment. This project has three aims. The first is to perform genome-wide RNAi screens on tumor-derived cell line models to identify tumor-specific vulnerabilities and understand the basis of therapy resistance to commonly used targeted therapies. Second is to probe the roles of breast cancer stem cells with emphasis on DNA methylation profiling. The third is to apply novel, focal re-sequencing methods developed in the laboratory to uncover genomic rearrangements that contribute to the susceptibility of breast cancer.

BODY

Fourth-generation (V4)RNAi resources

During this past year, we have completed the development of our shRNA prediction algorithm called shERWOOD. Prior algorithms for predicting effective RNAi reagents have suffered from two drawbacks for designing shRNAs. First, they have been derived from a relatively small number of data points. Even the best algorithm had only used approximately 2500 measurements of knockdown, such that there were an extremely small number of effective sequences present for the algorithm to learn their properties. In contrast, approximately 250,000 measurements of shRNA efficacy were used to train the shERWOOD algorithm. Second, until now, existing algorithms predict siRNAs, but not shRNAs. shRNAs have more sequence constraints than siRNAs due to their requirement for efficient processing by the cell's RNAi machinery. All effective RNAi prediction tools tend to choose sequences that begin with a U. This is thought to have a structural basis in the interaction between the RNA and Argonaute, the core of the RNAi effector complex. The 5' residue of the RNA has been shown to reside in a binding pocket which favors interaction with U. However, when the small RNA interacts with Argonaute, its 5' end is not available for pairing with the target RNA. Even though the 5' U contributes to RISC binding, it is irrelevant to target recognition. Thus we tested the idea that we could expand available sequence space by predicting on every position in the transcriptome and changing the small RNA guide that would pair to that site so that it began with a 5' U. This is henceforth referred to as the "1U-strategy". Simulation of this 1U-strategy compared to the same predictions lacking 1U produced higher potency scores for 1U constructs. Importantly, this improvement also enabled predictions on small genes with a limited number of potential target sequences.

To experimentally validate the 1U-strategy, we performed our 'sensor' assay using a library which targeted a set of 2000 genes ("druggable") with the top 15 predicted shRNA per gene. The sensor constructs contained target sites with the endogenous base, while the shRNAs were either with or without the 1U conversion. Our sensor assay screens for highly potent shRNAs in a highly parallel and high-throughput fashion. Distribution of the data indicated that approximately 50% of all the shRNAs were strong or very strong (knockdown efficiency >75%). When the native and artificial 1U shRNA data were plotted with their score distributions, we observed a significant reduction in efficacy of the non-native 1U shRNAs. We therefore stratified the 1U shRNAs based on their endogenous 5' nucleotide and found that only a subset of shRNAs performed well (endogenous 1U shRNAs) when a 1U-switch was made. Using this dataset, a new shERWOOD algorithm module was developed that could select for the strongest endogenous 1U shRNAs and identify which endogenous 1C, 1G, and 1A shRNAs are likely to yield potent 1U-converted molecules.

Since the previous update, we completed the construction of the human V4 library, which now has 88,275 shRNAs targeting 18,651 genes (with 16,681 genes represented by at least three shRNAs, 1,518 genes with at least two shRNAs, and 452 genes with one shRNA per

gene). The mouse V4 library currently has 58,113 shRNAs in total, targeting 18,769 genes (with 11,936 genes with three or more shRNAs).

RNAi screening of breast cancer cell line models for new therapeutic targets

Approximately 20% to 25% of invasive breast cancers exhibit overexpression of the human epidermal growth factor receptor (HER2) tyrosine kinase receptor. As elevated HER2 levels are associated with reduced disease-free and overall survival in metastatic breast cancer, therapeutic strategies have been developed to target this oncoprotein. Trastuzumab, a recombinant humanized monoclonal antibody directed against an extracellular region of HER2, was the first HER2-targeted therapy approved for treatment of HER2-overexpressing metastatic breast cancer. This drug is active as a single agent and in combination with adjuvant chemotherapy (either in sequence or in combination) in HER2-positive breast cancers. However, the objective response rates to trastuzumab mono-therapy were low (12% to 35%), and for a median duration of nine months, suggesting a majority of HER2-overexpressing tumors demonstrated *de novo* resistance. Phase III trials revealed that the combination of trastuzumab and paclitaxel or docetaxel could increase response rates, time to disease progression, and overall survival compared to trastuzumab mono-therapy. For HER2-positive patients who had not received prior chemotherapy, the median time to progression in response to trastuzumab as single-agent was less than five months. In patients who received trastuzumab and chemotherapy, the median time to progression was 7.5 months. Thus, the majority of patients who achieve an initial response to trastuzumab-based regimens develop resistance within one year. Elucidating the molecular mechanisms underlying acquired resistance to trastuzumab is essential for improving the survival of HER2-positive, metastatic breast cancer patients.

Our goal is to uncover mechanisms underlying the basis of acquired trastuzumab resistance and to find genes that can be targeted pharmacologically to reverse drug resistance. We have obtained several tumor-derived cell line models of acquired trastuzumab resistance from Dr. Dennis Slamon (UCLA). We performed genome-wide shRNA screens using our 3rd-generation human shRNA library in the presence and absence of trastuzumab to uncover shRNAs that would sensitize the resistant cell lines to the drug.

Status of genome-wide RNAi screens on HER2-positive, trastuzumab resistance (acquired) models:

<u>Cell line</u>	<u>Screening condition</u>	<u>Status</u>
SKBR3 (drug sensitive)	No drug	Screen completed. Samples sequenced. Data analyzed.
SKBR3 (drug sensitive)	Trastuzumab 15ug/ml	Screen completed. Samples sequenced. Data analyzed.
SK-TR (drug resistant)	No drug	Screen completed. Samples sequenced. Data analyzed.
SK-TR (drug resistant)	Trastuzumab 15ug/ml	Screen completed. Samples sequenced. Data analyzed.
EFM192A (drug sensitive)	No drug	Screen completed. Samples sequenced. Data analyzed.
EFM192A (drug sensitive)	Trastuzumab 15ug/ml	Screen completed. Samples sequenced. Data analyzed.
EFM-TR (drug resistant)	No drug	Screen completed. Samples sequencing in progress.
EFM-TR (drug resistant)	Trastuzumab 15ug/ml	Screen completed. Samples sequencing in progress.

To identify genes conferring secondary (acquired) resistance to trastuzumab from the datasets, we set a cutoff of $FDR < 0.25$ and filtered for genes that depleted only upon trastuzumab treatment in the drug resistant line, SKTR, but not in either of the two drug sensitive lines, SKBR3 and EFM192A. This produced a list of 25 genes (Figure 1: Heatmap of the 25 genes), which included those from PI3K-mTOR signaling (PI4K2A, Raptor, Insulin receptor, and EIF4A), RNA processing (PRPF8, U2AF1, and LSM6), mitotic checkpoint (BUB1B), and genes of relatively less well-known function. Identification of the insulin receptor and members of the PI3K-mTOR signaling pathway fulfills our expectation of finding these genes in this screen since they are known to be functionally associated with trastuzumab

resistance. However, TNFSF11/RANKL (ligand of the receptor activator of nuclear factor kappa B), a gene of significant relevance to breast cancer, was also found in the screen as one of two most highly depleted hits.

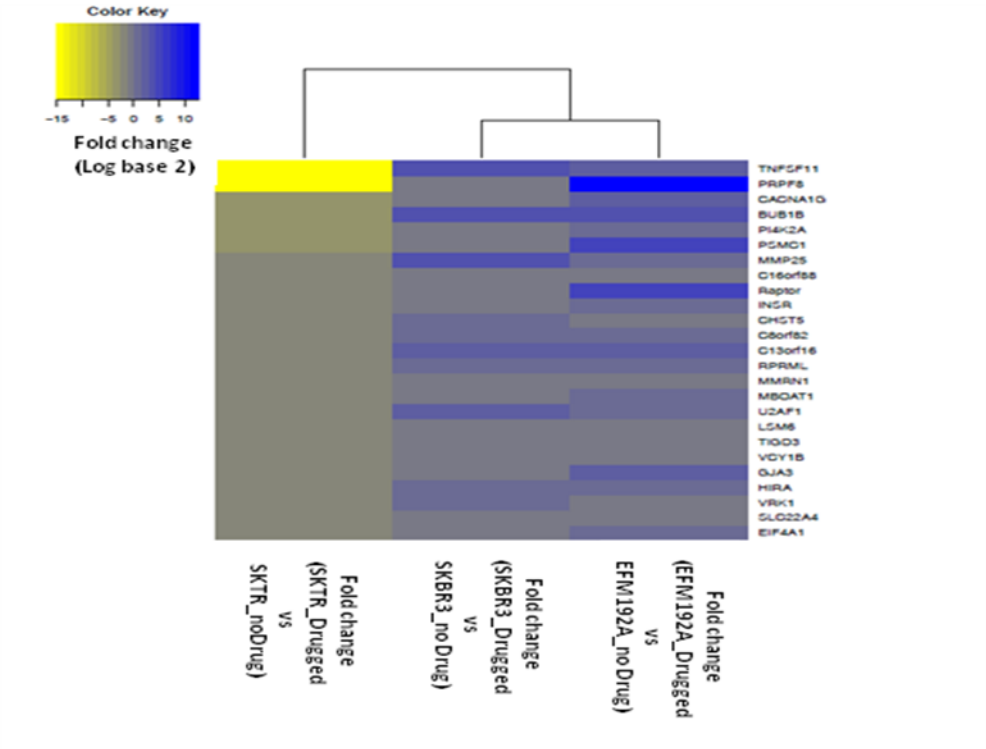


Figure 1.Heatmap of shRNAs (FDR<0.25) for gene targets that sensitize drug resistant (SKTR) and not drug sensitive cell line models (SKBR3 and EFM192A). These are potentially novel candidates for trastuzumab combination therapy.

Figure 2. Competition assays to validate selected hits. Cell line: SKTR (Drug resistant), Drug = Trastuzumab.

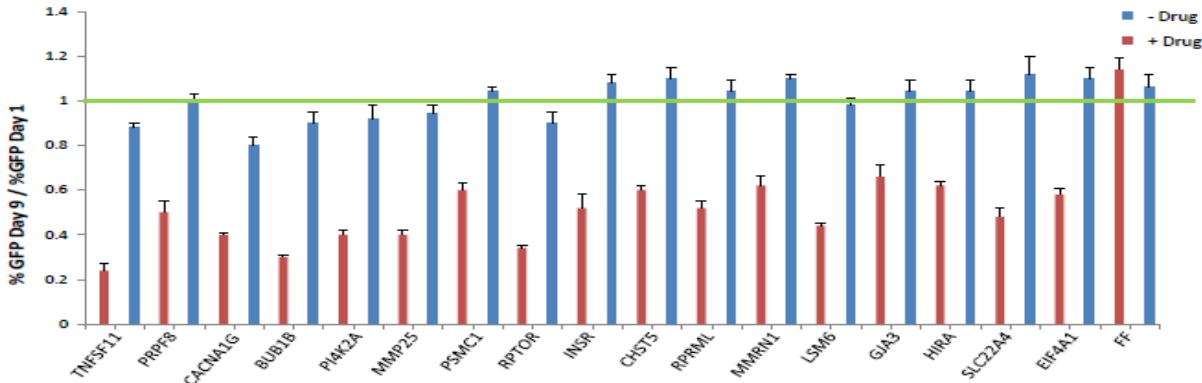
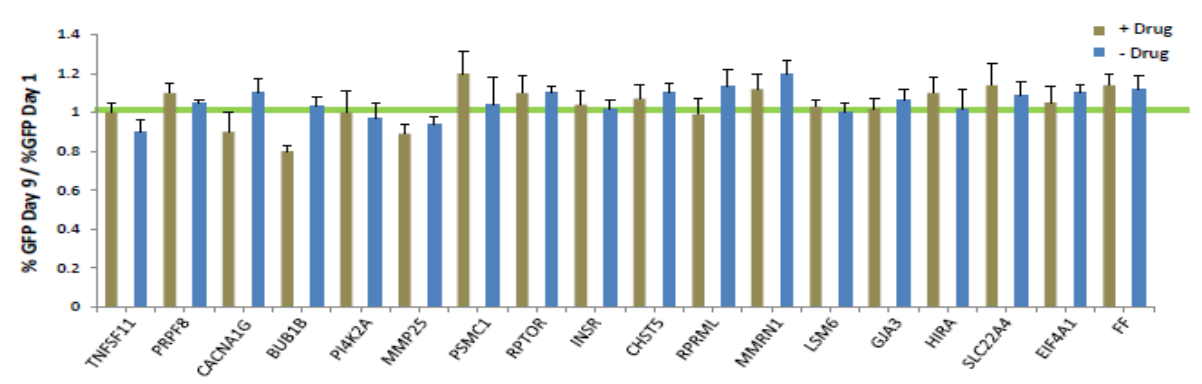


Figure 3. Competition assays to validate selected hits. Cell line: SKBR3 (Drug Sensitive), Drug = Trastuzumab.



We validated 17 of the 25 targets (Figure 1) by using competition assays and the results demonstrated that these target genes specifically sensitize the trastuzumab resistant cells (SKTR) when silenced by RNAi (Figure 2 and 3). In the competition assay, shRNA-expressing cells (GFP+) are mixed with an equal proportion of parental cells for each cell knockdown line. Each cell line mixture is plated in triplicate and either untreated or treated with drug. The percentage of GFP+ cells remaining is then tracked over time. We prioritized our effort by selection of RANKL/TNFSF11 as the first target for further validation due to the existence of a clinically approved inhibitor called Denosumab. Xenografts of these cell lines are currently being tested to validate whether RANKL is a target for trastuzumab sensitization *in vivo*. Ultimately, our goal is to test whether this combination approach will have an impact on reducing tumorigenicity in human breast cancer cells from patients that are resistant to trastuzumab therapy. In addition, we will continue to pursue the remaining targets in further validation studies.

Denosumab is a humanized monoclonal antibody designed to inhibit RANKL for treating various bone related conditions. This drug was approved for use to treat giant cell tumor of the bone, for breast cancer patients on adjuvant aromatase inhibitor therapy to increase bone mass, for postmenopausal women with risk of osteoporosis, and for the prevention of skeletal-related events in patients with bone metastases from solid tumors. Denosumab is highly specific as it binds human RANKL, but not murine RANKL, human TRAIL, or other human TNF family members. RANKL and its receptor RANK are best known for their essential function in bone remodeling and bone-related pathologies including osteoporosis and arthritis. The dysregulation of the RANKL-RANK system is the major cause of osteoporosis in post-menopausal women. Appropriate RANKL signaling is also required for the formation of a lactating mammary gland, and both RANKL and RANK are expressed under the control of progesterone, prolactin, and the parathyroid hormone protein-related peptide (PTHrP). Recent data also implicate RANKL and RANK in the control of metastasis of breast cancer cells to the bone and sex hormone-driven primary mammary cancer. Unfortunately, synthetic progesterone derivatives (progestins), such as medroxyprogesterone acetate (MPA), used in hormone replacement therapy and contraceptives have been demonstrated to induce the RANKL-RANK system, providing growth and survival advantage to damaged mammary epithelium, a requisite for tumor initiation. In addition, recent evidence links Her2 expression to RANKL-RANK signaling. Her2 expression is increased in luminal tumor cells grown in mouse bone xenografts, as well as in bone metastases from patients with breast cancer as compared to matched primary tumors. The increase in Her2 protein levels was not due to gene amplification, but rather was mediated by RANKL in the bone environment.

Epigenetic characterization of the mammary epithelial lineage

We have undertaken a full epigenetic characterization of the mouse mammary epithelial lineage from nulliparous and parous mice. Our goal is to understand how DNA methylation patterns change as cells differentiate along this lineage and understand what discriminates stem cells from their mature progeny. This work has subsequently resulted in a publication¹ of which a reprint is attached to this report. Please refer to this article for detailed descriptions of specific aspects of the research.

KEY RESEARCH ACCOMPLISHMENTS

- Development of a shRNA prediction algorithm (shERWOOD) that essentially predicts the results of functional, sensor testing of shRNAs *in silico*.
- Completed construction of a sequence-verified, human, 4th-generation shRNA resource.

- Discovery of potential target genes to sensitize Her2-positive, trastuzumab-resistant cell models of breast cancer.
- Defining the molecular hierarchy of mammary differentiation yielded refined markers of mammary stem cells.

REPORTABLE OUTCOMES

- Developed a shRNA-specific prediction algorithm, called shERWOOD.
- Completed construction of a 4th-generation, human shRNA library consisting of 88,275 shRNAs and targeting 18,651 genes (with 16,681 genes represented by at least three shRNAs).
- Constructed and sequence-verified 58,113 shRNAs (targeting 18,769 genes) of the 4th-generation, mouse shRNA library.
- Both human and mouse 4th-generation shRNA resources are available to the scientific community through Transomic Technologies Inc. (Huntsville, Alabama).
- Published manuscript:
 “Molecular hierarchy of mammary differentiation yields refined markers of mammary stem cells”
 Camila O. dos Santos, Clare Rebbeck, Elena Rozhkova, Amy Valentine, Abigail Samuels, Lolahon R. Kadiri, Pavel Osten, Elena Y. Harris, Philip J. Uren, Andrew D. Smith, and Gregory J. Hannon.
PNAS (2013), 110(18):7123-7130.

CONCLUSION

We are continuing to make progress towards our aims in the proposal. During this past year, we have had some very promising outcomes with the completion of the human shRNA library and with most of the mouse shRNA library completed. A new shRNA algorithm for predicting sensor-verified shRNAs have been developed. New mammary epithelial stem cell markers have been identified with implications toward breast cancer development.

REFERENCES

1. Dos Santos C.O., Rebbeck R., Rozhkova E., Valentine A., Samuels A., Kadiri L.R., Osten P., Harris E.Y., Uren P.J., Smith A.D., Hannon G.J. (2013), *PNAS* 110(18):7123-7130.

Molecular hierarchy of mammary differentiation yields refined markers of mammary stem cells

Camila O. dos Santos^{a,1}, Clare Rebbeck^a, Elena Rozhkova^a, Amy Valentine^a, Abigail Samuels^{a,b}, Lolahon R. Kadir^c, Pavel Osten^c, Elena Y. Harris^{d,2}, Philip J. Uren^d, Andrew D. Smith^d, and Gregory J. Hannon^{a,1}

^aHoward Hughes Medical Institute, Cold Spring Harbor Laboratory, Cold Spring Harbor, NY 11724; ^bArts and Science Undergraduate Program, Vanderbilt University, Nashville, TN 37212; ^cCold Spring Harbor Laboratory, Cold Spring Harbor, NY 11724; and ^dMolecular and Computational Biology, University of Southern California, Los Angeles, CA 90089

This contribution is part of the special series of Inaugural Articles by members of the National Academy of Sciences elected in 2012.

Contributed by Gregory J. Hannon, March 11, 2013 (sent for review December 28, 2012)

The partial purification of mouse mammary gland stem cells (MaSCs) using combinatorial cell surface markers (Lin[−]CD24⁺CD29^hCD49^f) has improved our understanding of their role in normal development and breast tumorigenesis. Despite the significant improvement in MaSC enrichment, there is presently no methodology that adequately isolates pure MaSCs. Seeking new markers of MaSCs, we characterized the stem-like properties and expression signature of label-retaining cells from the mammary gland of mice expressing a controllable H2b-GFP transgene. In this system, the transgene expression can be repressed in a doxycycline-dependent fashion, allowing isolation of slowly dividing cells with retained nuclear GFP signal. Here, we show that H2b-GFP^h cells reside within the predicted MaSC compartment and display greater mammary reconstitution unit frequency compared with H2b-GFP^{neg} MaSCs. According to their transcriptome profile, H2b-GFP^h MaSCs are enriched for pathways thought to play important roles in adult stem cells. We found Cd1d, a glycoprotein expressed on the surface of antigen-presenting cells, to be highly expressed by H2b-GFP^h MaSCs, and isolation of Cd1d⁺ MaSCs further improved the mammary reconstitution unit enrichment frequency to nearly a single-cell level. Additionally, we functionally characterized a set of MaSC-enriched genes, discovering factors controlling MaSC survival. Collectively, our data provide tools for isolating a more precisely defined population of MaSCs and point to potentially critical factors for MaSC maintenance.

FACS sorting | mammary gland transplant | shRNA screen

The murine mammary gland resembles, to some extent, the human mammary gland in development, milk production, and progression to carcinogenesis, making it an ideal system to develop methodologies and form hypotheses of relevance to women. The use of cell surface markers to isolate selected cell types from mice has greatly enhanced our understanding of development and our knowledge of molecular pathways and interactions that influence it. Mammary gland stem cells (MaSCs) have commanded attention because of not only their roles in the cycles of gland morphogenesis but also their potential contribution in tumor initiation. Full characterization of MaSCs, however, has been hampered by their scarcity. Enrichment of the MaSC compartment has, until now, been achieved by using a combination of cell surface markers (Lin[−]CD24⁺CD29^hCD49^f) (1, 2). Thus far, these cells have been enriched to 1 MaSC per every 64 cells stained Lin[−]CD24⁺CD29^h (1). This is sufficient to test for MaSC repopulation capacity and to some extent, roles in tumorigenesis, but this level of purity is less suitable for more complex molecular analyses that define MaSCs and their properties.

Additional characterization of MaSCs has been achieved using a transgenic mouse model expressing GFP under the control of the *s-ship* promoter (3). This gene is expressed in embryonic and hematopoietic stem cells but not differentiated cells (4). GFP⁺ cells in this mouse model were shown to reside at the tips of the terminal end buds, where MaSCs are believed to be located in these

developing mammary gland structures (3, 5). Transplantation of the MaSC-enriched GFP⁺CD49^f cells improved the mammary reconstitution unit (MRU) frequency to 1/48 cells, an increase over the previous shown frequency for CD24⁺CD29^hCD49^f cells. Although being very elegantly performed and enhancing our understanding of MaSC localization, studies with this mouse model did not achieve a greater enrichment for MaSCs using more conveniently accessible markers, such as cell surface proteins.

Given the limitations in accurately purifying MaSCs, we sought to devise a method better suited for identifying this population. Here, we describe the use of long-term label retention to increase the MRU frequency within MaSC-enriched CD24⁺CD29^h cells. This approach, previously applied to the isolation of skin stem cells (6), enables the identification of slowly dividing cells, a characteristic of adult stem cells. To mark slowly dividing cells, expression of the H2b histone, linked to GFP, is regulated by a tetracycline responsive element (TRE) and a tet-controlled transcription activator (tTA) under the endogenous keratin K5 promoter (K5tTA-H2b-GFP). In the absence of tetracycline or its analog doxycycline (DOX), the tTA binds to TRE and activates transcription of H2b-GFP. Treatment with DOX prevents the tTA binding to TRE, and transcription of H2b-GFP is terminated (6). As the cell divides, newly synthesized, unlabeled H2b replaces the H2b-GFP; therefore, the more slowly dividing cells will retain GFP expression for an extended period.

We were able to improve the MaSC enrichment by isolating GFP-retaining cells after a long-term inhibition of transgene expression. We refer to these cells as H2b-GFP^h MaSCs (CD24⁺CD29^hH2b-GFP^h). Comparisons between expression profiles of all mammary gland cell types suggested that H2b-GFP^h MaSCs differentially expressed several genes involved in pathways previously described as playing roles in other adult stem cells. Additional analysis of the H2b-GFP^h MaSC expression signature led to the identification of a cell surface marker that, combined

Author contributions: C.O.d.S. and G.J.H. designed research; C.O.d.S., E.R., A.V., A.S., L.K., and P.O. performed research; C.O.d.S., E.Y.H., P.J.U., and A.D.S. analyzed data; and C.O.d.S., C.R., and G.J.H. wrote the paper.

The authors declare no conflict of interest.

Freely available online through the PNAS open access option.

Data deposition: The sequences reported in this paper have been deposited at the National Center for Biotechnology Information Short Read Archive (NCBI SRA) [submission study [SRR018968](https://www.ncbi.nlm.nih.gov/sra/SRR018968) regarding the following samples: Myo differentiated SRX246984 (SRR768419 and SRR768420); Myo progenitor SRX246985 (SRR768421 and SRR768422); luminal alveolar SRX246986 (SRR768423 and SRR768424); luminal progenitor SRX246987 (SRR768425 and SRR768426); luminal ductal SRX246988 (SRR768427 and SRR768428); H2b GFP MaSC SRX246989 (SRR768429, SRR768430, and SRR768431); CD59 MaSC SRX246990 (SRR768432); and CD1d MaSC SRX246991 (SRR768433)].

¹To whom correspondence may be addressed. E-mail: dossanto@cshl.edu or hannon@cshl.edu.

²Present address: Computer Science Department, California State Polytechnic University, Pomona, CA 91768.

This article contains supporting information online at www.pnas.org/lookup/suppl/doi:10.1073/pnas.1303919110/-DCSupplemental.

with conventional markers, resulted in the isolation of an MaSC population with an elevated proportion of MRUs. In addition, we performed a focused shRNA screen, targeting genes that were differentially expressed in our newly characterized MaSC-enriched cell population, revealing potential regulators of mammary gland biogenesis. Overall, this work improves our ability to purify MaSCs and provides valuable insights into their role in mammary gland development and perhaps, even tumor initiation.

Results

H2b-GFP Label-Retaining Cells Enrich for MaSCs. To better enrich for the MaSC population, we assessed the feasibility of using mammary gland label-retaining cells to select for MaSCs, given that a slower division rate is an expected characteristic of adult stem cells. We adopted a system wherein expression of the H2b histone, linked to GFP, is regulated by a TRE and a tTA under the endogenous keratin K5 promoter K5tTA-H2b-GFP (a gift from Elaine Fuchs, Rockefeller University, New York, NY). Keratin K5 is expressed in cells of the basal compartment, the region considered to be home to MaSCs (7). This system displays some advantages over the previous gene reporter-based methods used to isolate MaSCs, because it takes advantage of one of the more general properties of stem cells: their relative quiescence. In support of the use of this mouse model, there were previous hints that MaSC-enriched CD24⁺CD29^h cells display BrdU label-retaining properties (1), although label-retaining populations were not functionally characterized.

Initial experiments using the H2b-GFP mice assessed the expression and distribution of GFP-positive cells in the adult mammary gland (Fig. 1A). Histological sections revealed the presence of several GFP⁺ cells located within structures resembling the mammary gland ductal epithelium (Fig. 1B and Fig. S1A, Upper). Treatment of H2b-GFP mice with DOX over a 12-wk period, thus ceasing transcription of H2b-GFP transgene, dramatically reduced the number of cells expressing GFP. Notably, those cells that remained GFP⁺ were located at the tips of the terminal end buds. These distinct sites in the ductal epithelium are the areas currently believed to be resident by MaSCs (8) (Fig. 1C and Fig. S1A, Lower).

To compliment this observation, under the hypothesis that mammary gland label-retaining cells comprise a population of potential MaSCs, we investigated the correlation between GFP retention and expression of previously defined MaSC-enriched cell surface markers, CD24 and CD29. Using FACS analysis, we were able to subdivide the mammary gland (after depletion of endothelial and hematopoietic cells as shown in Fig. S1B) into three distinct cell compartments: luminal (CD24^hCD29⁺), occupied by luminal cells; basal (CD24⁺CD29^h), occupied by myoepithelial cells and MaSCs; and stromal (CD24[−]CD29⁺) (1) (Fig. 1D, Upper Left). The majority of GFP⁺ cells from a transgenic H2b-GFP mouse off DOX could be categorized into either basal or stromal compartments, with far fewer GFP⁺ cells occupying the luminal compartment (Fig. 1D, Upper Right and Fig. S1C, Left). After a 12-wk DOX chase, the overall proportion of GFP⁺ cells decreased by more than one-half, and the presence of a GFP⁺ luminal compartment was all but eliminated (Fig. 1D, Lower Left and Fig. S1C, Center). Focusing on GFP intensity (a measure that directly relates to the rate of cell division), selection of only the brightest GFP⁺ cells (GFP^h) resulted in a greater proportion remaining in the CD24⁺CD29^h basal compartment, whereas the stromal compartment was significantly reduced after GFP^{dim} cells were removed (Fig. 1D, Lower Right and Fig. S1C, Right). This result suggests that the most label-retaining cells reside within the basal compartment and may represent the MaSCs population.

The benefit of using GFP to test for label retention, as opposed to BrdU, is that its detection does not require fixation and staining. We were then able to test the biological differences,

using mammary gland transplants, between GFP^h cells (H2b-GFP^h MaSCs) and GFP[−] cells (H2b-GFP[−] MaSCs) within the MaSC-enriched compartment. Transplantation assays are a fundamental criterion to evaluate stemness and have been used previously for several tissues, including the mammary gland (1, 2, 9). For these experiments, the inguinal glands were removed from the endogenous tissue of prepubescent females before injection of donor cells. Donor cells were harvested from mammary glands of H2b-GFP mice after a 12-wk DOX chase, dissociated, lineage-depleted, and sorted according to GFP intensity (Fig. S1D). Cells (GFP^h and GFP[−]) were then injected, and outgrowths from donor cells were compared (by visualization of GFP⁺ epithelium) 12 wk posttransplantation. Given that the recipient animals are not treated with DOX, all cells derived from the donor mice will resume expression of the H2b-GFP transgene and give rise to GFP⁺ outgrowths. MRU frequency was estimated according to the previously described algorithm (10). Transplantation of 500 H2b-GFP^h MaSCs ($n = 5$) gave rise to GFP⁺ epithelium in all injected glands. This ability to reconstitute was still retained when only 50 cells were transplanted (Fig. 1E). In contrast, only one-half of the glands injected with 500 H2b-GFP[−] MaSCs displayed fluorescent outgrowths, decreasing to just 29% with injection of 50 cells (Dataset S1). These results represent an increase in the estimated frequency of MRUs from 1/70 cells, when MaSC selection was performed using CD24⁺CD29^h alone (1), to 1/33 cells, with restriction to H2b-GFP^h cells to further define MaSCs. Comparatively, the MRU frequency among H2b-GFP[−] MaSCs was estimated to be 1/149 (Dataset S1). Colony-forming ability was also twofold greater for H2b-GFP^h MaSCs when 500 of these cells were seeded in a Matrigel (BD Bioscience) and cultured for 7 d (Fig. S1E).

Considered together, these data suggest that mammary gland H2b-GFP^h label-retaining cells represent a subset, if not an entire population, of the MaSCs. Our experiments using a repressible H2b-GFP transgene have built on previous knowledge regarding the label-retaining properties of stem cells in the mammary gland and confirmed that MaSC CD24⁺CD29^h cells reside mainly within the H2b-GFP^h label-retaining cell population. In addition to these experiments, we also found that hormone-dependent activation of MaSC proliferation and differentiation, triggered by one complete cycle of pregnancy and involution in transgenic H2b-GFP mice treated with DOX, completely depleted GFP⁺ cells, validating that H2b-GFP^h cells truly represent a population of slowly dividing cells rather than being a transgenic artifact.

It has been proposed that MaSCs comprise less than 5% of the total basal compartment. Our findings support this notion given that we find label-retaining H2b-GFP^h cells to account for ~0.2% of the total CD24⁺CD29^h population (Fig. S1D, Upper Right). We also compared the distribution of H2b-GFP^h-retaining cells with expression of a recently identified marker for myoepithelial progenitor-like cells, CD61. This marker was expressed by most of the H2b-GFP^{dim} population, whereas virtually all H2b-GFP^h cells were negative for CD61 staining, suggesting perhaps a unique mammary gland cell differentiation pattern, where H2b-GFP^h label-retaining cells might occupy the top of hierarchy.

H2b-GFP Cells Display a Stem Cell-Like Expression Signature. Having established that H2b-GFP^h MaSCs have reconstitution properties, we next sought to determine where these cells fall in the mammary differentiation hierarchy with regard to their gene expression patterns. Using a combination of cell surface markers (1, 11), six distinct cell types were isolated by FACS to a purity of >90%: H2b-GFP MaSCs (Lin[−]CD24⁺CD29^hH2b-GFP^hCD61[−]), myoepithelial progenitor-like cells (Lin[−]CD24⁺CD29^hH2b-GFP^hCD61⁺), myoepithelial differentiated cells (Lin[−]CD24⁺CD29^hH2b-GFP[−]CD61[−]), luminal progenitor cells (Lin[−]CD24^hCD29⁺CD61⁺CD133[−]), luminal ductal cells (Lin[−]CD24^hCD29⁺CD61[−]CD133⁺), and luminal alveolar cells (Lin[−]CD24^hCD29⁺CD61[−]CD133[−]).

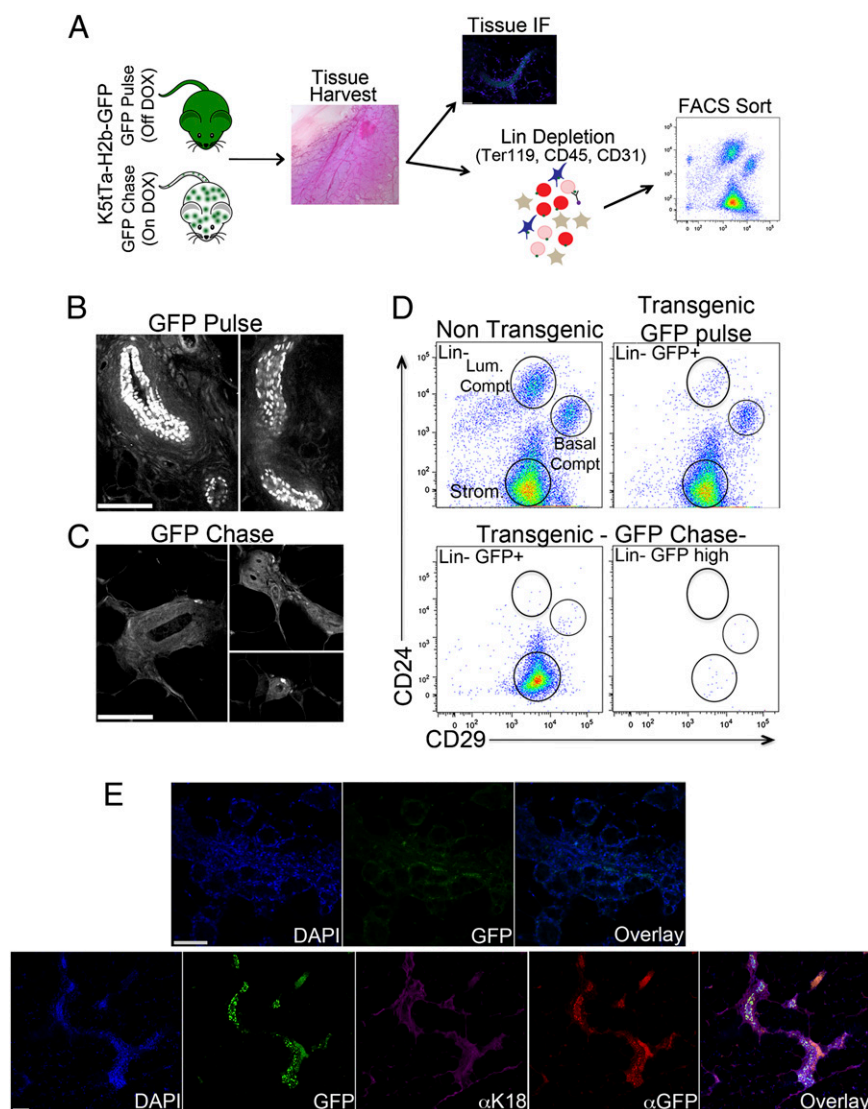


Fig. 1. H2b-GFP label-retaining cells represent a population of MaSCs. (A) Experimental scheme. Mammary glands were harvested from K5tTa-H2b-GFP transgenic mice either off (GFP pulse) or on DOX diet (GFP chase) and further processed for immunological staining or single-cell suspension FACS sorting. (B and C) Tissue histology H2b-GFP⁺ cells distribution. Mammary glands from transgenic mice off and on DOX diet were harvested, defatted, embedded in agarose, and imaged with two-photon microscopy. (B) Mice off DOX diet (GFP pulse) showing a broad distribution of GFP⁺ cells in mammary gland ductal structures. (C) After a 12-wk DOX chase, H2b-GFP⁺ label-retaining cells became restricted to the edges of the ductal structures. (D) Flow cytometry profile of H2b-GFP⁺ cells. *Upper Left* shows the profile of a lineage-depleted (CD45[−], Ter119[−], and CD31[−]) nontransgenic mammary gland according to CD24 and CD29 staining and highlights the three cell compartments: luminal (CD24⁺CD29⁺; comprising luminal progenitor cells, luminal alveolar cells, and luminal ductal cells); basal (CD24⁺CD29^h; comprising myoepithelial progenitor cells, myoepithelial differentiated cells, and MaSCs); and stromal. Total GFP⁺ cells from H2b-GFP transgenic mice off DOX diet (GFP pulse mice; *Upper Right*) displayed a similar cellular compartmental distribution with fewer luminal-type cells. The CD24CD29 cell profile of H2b-GFP⁺ cells from GFP chase mice (on DOX) were analyzed using two strategies to define GFP-expressing cells. *Lower Left* displays CD24CD29 staining of total H2b-GFP⁺ cells, whereas *Lower Right* shows the CD24CD29 staining of H2b-GFP^h cells. The focus on GFP^h cells, the most label-retaining cells, drastically decreased the cellular content of all mammary gland compartments and retained a greater proportion of cells inside of the basal compartment, potentially representing MaSCs. (E) Histological analysis of mammary gland H2b-GFP^h MaSCs outgrowths. Cleared fat pads from prepubescent female mice were injected with either total H2b-GFP[−] MaSCs (CD24⁺CD29^hGFP[−] cells) or H2b-GFP^h MaSCs (CD24⁺CD29^hGFP^h cells), harvested 12 wk after transplantation, embedded in agarose, stained with antibodies, and imaged on a Zeiss 710 LSM (Zeiss) confocal microscope. Images display outgrowths of two distinct glands injected with H2b-GFP^h MaSCs.

(Fig. 2A). The myoepithelial progenitor-like cells were defined by expression of CD61 as a positive cell surface marker and their positioning as the second most label-retaining cell population.

Hierarchical clustering of combined RNAseq replicates split mammary gland cells into two main branches: the basal compartment, comprising myoepithelial progenitor cells, myoepithelial differentiated cells, and H2b-GFP MaSCs, and the luminal compartment, with luminal progenitor cells and differentiated cells (Fig. 2B). As predicted by prior characterization of MaSCs (1), we found the expression profile of H2b-GFP MaSCs to be

more closely related to the expression profile of myoepithelial cells than luminal cells; however, H2b-GFP MaSCs were still an out-group compared with other cells in this cluster. Analysis over all mammary gland cell types yielded several hundred genes differentially expressed among all cell types (Fig. 2B), spanning diverse gene ontology groups and pathways (Dataset S2). More specifically, genes differentially expressed in H2b-GFP MaSCs were enriched in G protein-coupled receptors and pathways involving Wnt/B-catenin signaling, areas previously described to play fundamental roles in other adult stem cells (12). Differential

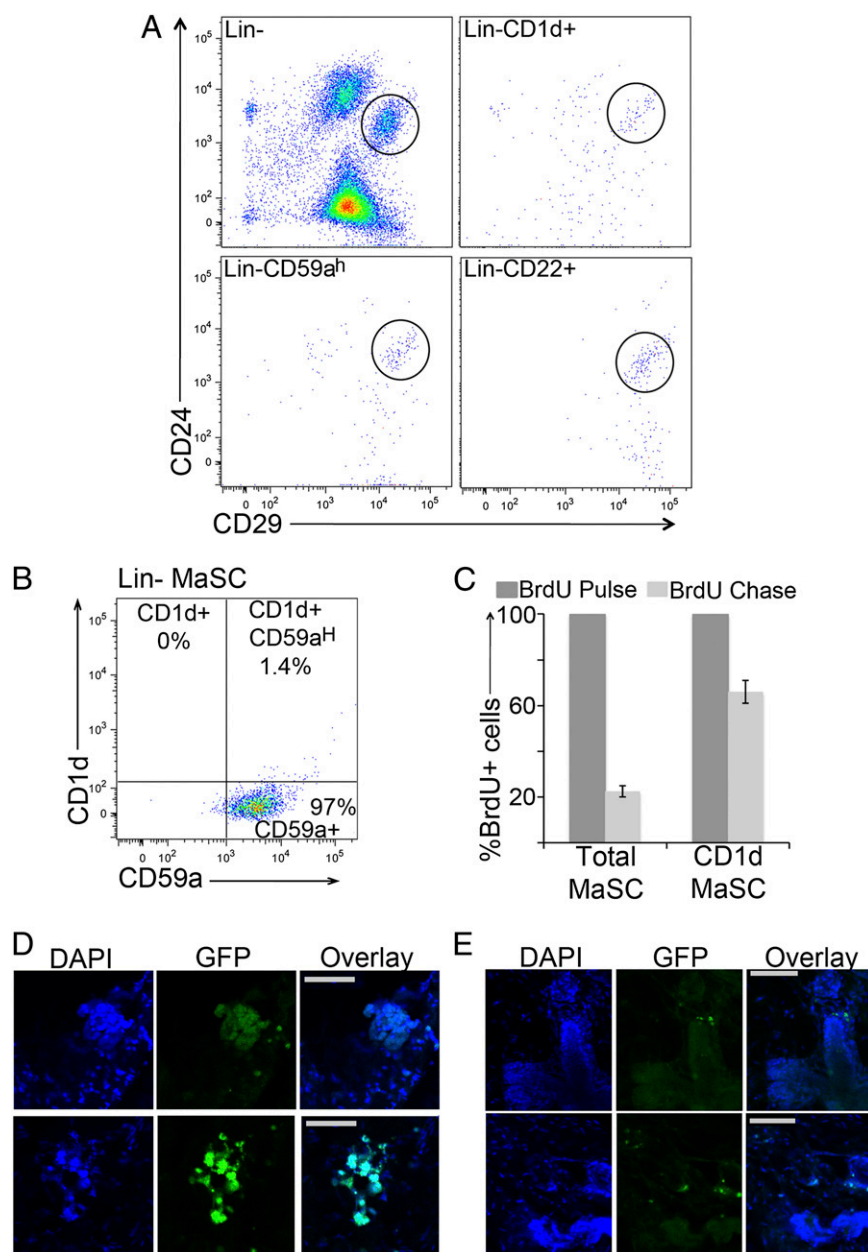


Fig. 3. CD1d is an additional cell surface marker for purification of MaSCs. (A) FACS analysis of MaSC cell surface markers. Total MaSCs (CD24⁺CD29^h cells) were additionally segregated according to the expression of the cell surface markers CD1d, CD59a^h, or CD22. (B) CD1d is expressed by a subset of CD59a^h cells. Lin⁻ mammary gland cells were stained with antibodies against CD24, CD29, CD1d, and CD59a and further analyzed on an LSRII Cell Analyzer (BD Bioscience). The entire basal compartment (CD24⁺CD29^h) was selected and analyzed according to CD1d and CD59a expression. The majority of cells within the basal compartment stained positive for CD59a, and CD1d⁺ cells fell mainly in the CD59a^h area. (C) CD1d MaSCs are the most label-retaining cells within the mammary gland. Prepubescence mice were injected with BrdU (50 mg/kg body weight) for 5 d. Glands were either harvested from mice on the last day of BrdU injection to evaluate the total BrdU incorporation (week 0) or harvested after a 12 wk BrdU chase. Single-cell suspensions were stained with antibodies against CD24, CD29, and CD1d and analyzed on an LSRII Cell Analyzer (BD Bioscience). BrdU incorporation was measured in total MaSC (CD24⁺CD29^h) and CD1d MaSC (CD24⁺CD29^hCD1d⁺) populations. (D and E) Histological analysis of mammary gland CD1d MaSCs outgrowths. Cleared fat pads from prepubescent female mice were injected with (D) either total MaSCs or CD1d MaSCs and (E) 25 CD1d MaSCs cells harvested from glands pretransplanted with CD1d MaSCs. Glands were harvested 12 wk after transplantation and embedded in agarose, and endogenous GFP signal was imaged. Images display outgrowths from two distinct glands injected with CD1d MaSCs cells (D) or secondary transplanted CD1d MaSCs (E).

shRNAs were introduced into the immortalized mammary gland cell line, Comma-D β (18). These cells give rise to both luminal and myoepithelial compartments in colony-forming and transplantation assays, independent of the method of MaSC enrichment (19–21). In addition, ~50% of Comma-D β cells stain positive for Cd1d, placing them in our improved MaSCs isolation profile (Fig. S4B).

Cells were monitored for GFP expression (as a proxy for shRNA expression), and changes in the proportion of GFP-expressing cells would be indicative of a relevant gene function. The majority of screened shRNAs did not alter GFP levels during the 3-wk screening period (Fig. 4A), which could suggest that the correspondent genes were not essential for growth maintenance of Comma-D β cells. However, a distinct set of shRNAs altered

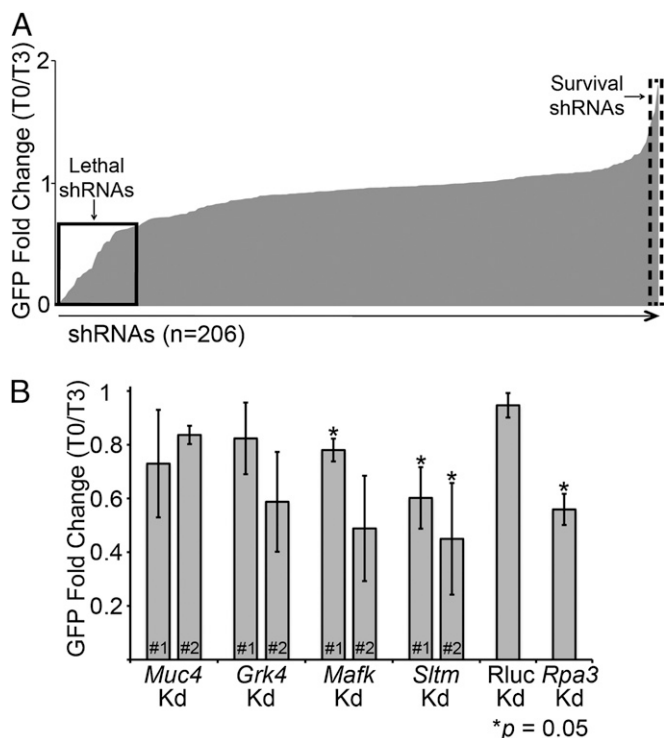


Fig. 4. Mammary gland focused screen. (A) One by one screen; 206 shRNAs, covering ~56 genes, were tested. The solid line square shows the fold change of shRNAs considered to be lethal, because GFP percent for these cells decreased overtime, whereas the dashed line square highlights data from shRNAs considered to show survival preferences in cells, because GFP percent increased overtime. (B) Screen hits validation. Two new hairpins targeting four genes selected as lethal hits from the first screen. The chart represents results of two independent experiments. * $P = 0.05$ by the t test.

the maintenance of GFP-expressing cells by either depleting GFP⁺ cells (Fig. 4A, lethal shRNAs) or promoting expansion of GFP⁺ cells (Fig. 4A, survival shRNAs) over time.

We decided to further investigate a subset of genes that interfered with Comma-D β growth, because our focus was to understand the spectrum of genes that might block normal mammary gland biogenesis. Among the selected genes were mucin-like gene (*Muc4*), G protein-coupled receptor gene family member (*Grk4*), and transcription factors (*Mafk* and *Sltn*). An additional set of hairpins for these genes was rescreened in Comma-D β cells with GFP levels followed for 10 d. No clear effect on the percentage of GFP-positive cells was observed when cells expressed the new shRNAs against *Muc4* and Renilla luciferase control, whereas an shRNA-dependent response was observed, according to GFP frequency, when the genes *Grk4* and *Mafk* were targeted (Fig. 4B). In addition, both new shRNAs against the gene *Sltn* consistently decreased GFP-expressing cells to levels comparable with the depletion achieved by *Rpa3*, the lethal control. Interestingly, *Sltn* encodes a transcription factor-like protein that binds both DNA (scaffold attachment factor-box DNA binding motif) and RNA (RNA binding domain) in response to estrogen levels (22). We are currently investigating the implications caused by loss of *Sltn* expression during normal mammary gland development and tumorigenesis.

Discussion

The ongoing interest in stem cells and more recently, cancer stem cells highlights the need for improvements in purification and analysis of this rare but important population. Our previous understanding of MaSCs has been clouded by the limited

capability to obtain a pure population devoid of contaminating, more differentiated cells. Here, we took advantage of a previously used system to identify relatively quiescent cells (6) in the mammary gland. We propose that the label-retaining cells from the K5tTa-H2b-GFP mouse represent a subset of active MaSCs, displaying increased mammary gland reconstitution ability over previously published cell populations identified as MaSCs.

Unlike previous methods, where cell selection is based on the presence of constitutive fluorescence in cells (3, 23), the use of a cell state-dependent GFP system allows for a more biological relevant fluorescence reliability. The extended time between halting GFP expression and analysis and also, selection of only the brightest cells decrease the possibility that the GFP protein might be detected in a cell cycling at a normal rate, despite the fact that the GFP expression is switched off. This system allowed for the possibility of a much more stringent selection process; however, it is acknowledged that there are limitations with using this mouse model on a routine basis for enriching for MaSCs. The need to use a transgenic mouse and however reduced, the level of heterogeneity within cells selected—evident by <100% regrowth efficiency—illustrate the need for the cell surface marker, CD1d, identified in our study.

CD1d is known to be expressed as a cell surface marker on a variety of antigen-presenting cells belonging to a cluster of glycoproteins involved in T-cell antigen presentation (13). Because we physically remove all hematopoietic cells using magnetic beads before FACS, we are confident that this differentially expressed marker does not simply reflect contaminating cells. This statement is supported by the presence of CD1d⁺ cells within the normal-like mammary gland cell line, Comma-1D β . In fact, 50% of these cells, isolated during midpregnancy, were positive for CD1d when stained with two distinct antibodies (Fig. S4B).

We, therefore, propose that CD1d is a genuine marker for MaSCs and when used combined with the cell surface markers CD24 and CD29, greatly enhances the purification of reconstituting cells above and beyond those cells selected based on label retention alone and those selected based on previously published markers. We perhaps did not exhaust all of the possibilities presented by our RNAseq data for the description of novel MaSC markers, but our findings do support CD1d as being a valuable component for purifying true MaSCs.

We found the proportion of CD1d⁺ cells (1%) within the basal compartment to be greater than the proportion of H2b-GFP^h cells (0.2%) in this same compartment. This observation draws to light another drawback of relying solely on this particular label-retaining mouse model and in the same context, relying on GFP expression of a gene reporter mouse to identify MaSCs. The cytokeratin K5 (*Krt5*), for example, although shown to be expressed by basal-type cells, may not be expressed by all cells in this compartment. In addition, GFP expression may also be disrupted in some cells, perhaps by suppression of the transgene promoter; alternatively, some cells could fail to shut down GFP expression on DOX treatment. Had we only selected cells based on GFP expression from the K5 promoter, we would not be selecting all—or solely—those cells capable of self-renewal. This exclusion of MaSCs has been illustrated previously, where cells negative for a reporter GFP were able to still proliferate and regenerate into a new gland (3), something that we also see to a small degree with the K5tTa-H2b-GFP mouse model.

The identification of CD1d as a unique marker for this MaSC population and the distinct transcriptome of the Cd1d MaSCs suggest that these cells perform a function distinct from progenitors and more differentiated cells. Despite their gene expression profile clustering more closely with myoepithelial cells, they are still able to produce a new gland. It is unclear, however, if all of the CD1d MaSCs are multipotent stem cells or if they represent a combination of the recently described luminal and

myoepithelial unipotent MaSCs (23). Because we are not using lineage tracing here, we cannot say for certain if all of the injected CD1d MaSCs would give rise to both compartments when allowed to repopulate the gland and if they are themselves the precursors to the cells that are largely responsible for tissue maintenance.

Identifying the genes involved in maintaining a stem cell and their self-renewing capabilities is vital to furthering our understanding of how these genes might be involved in abnormal gland development and tumorigenesis. Our current knowledge on this hypothesis, however, is, at best, limited; until now, it has been difficult to segregate myoepithelial cells and MaSCs, because they share common cell surface markers and very similar gene expression profiles (1, 24). The large number of shared genes expressed among cells identified by standard markers would mask any true differential patterns expressed by those cells with self-renewing properties. CD1d MaSCs cells only become divergent when the expression patterns of a relatively small number of genes are considered, a fact that would be overlooked if not using a more refined selection process. In addition to improving gene profiling as a whole for this minority population, the use of CD1d to isolate single cells for profiling could provide clues to gene expression changes between hypothesized MaSC states. For example, the complete loss of label-retaining cells after pregnancy suggests that these cells have undergone a more extensive process of cell division than in a virgin gland. However, CD1d⁺ cells are still present, unaltered to some extent, and using this marker, it would be possible to monitor gene expression changes during pregnancy and involution.

It has been suggested that stem cells within the mammary gland contribute in some way to the proposed notion of a cancer stem cell. In mouse mammary tumor virus (MMTV)-Wnt1 and p53^{-/-} mice, for example, a preneoplastic mammary gland was seen to have an increased number of functional MaSCs, and ectopic expression of wnt-1 enhanced the self-renewing capabilities of cells, leading to cancers (24). CD1d itself has even been linked to breast cancer. In one study, antibodies against CD1d, combined with anti death receptor 5 (anti-DR5), a TNF-related apoptosis inducing ligand (TRAIL) receptor, led to rejection of tumor growth after injection of 4T1 tumor cells, a mouse breast cancer cell line (25), into a syngeneic mouse fat pad (26). Whether this observation was a result of the proposed interaction with natural killer cells or a disruption of the ability of the cancer to self-renew remains to be seen. The latter could be possible, because we show that the 4T1 mouse breast cancer cell line (Fig. S4C) and primary mouse breast cells (27) (Fig. S4D) display a population of cells that is positive for Cd1d. In humans as well, CD1d plays some unknown role. Down-regulation of CD1d expression has been shown to correlate with increasing metastasis in a mouse breast cancer model (28) and disease progression in multiple myeloma (29). Our own studies have shown that CD1d is expressed as a cell surface marker in some but not all of the human breast cancer cell lines tested (Fig. S4E). Those cell lines that showed CD1d⁺ cells were from basal-like breast cancers; luminal-like cancer cell lines, however, showed no CD1d⁺ cells.

With the ability to now purify a more homogeneous self-renewing population of MaSCs, it is possible to delve more deeply into the biology of these cells. We have not only appointed CD1d as a marker of MaSCs but also used this information to draw out gene targets for disrupting mammary gland development and possibly, malignancies. It is also unknown yet if these specific cell markers are a cause or effect of the ability of the cell to retain stemness; interrupting their expression and studying the effect on gland development and cancer are critical topics of future study.

Materials and Methods

Mice. K5Ta-H2b-GFP heterozygote mice (6) were bred, and 20-d-old pups were checked for GFP expression using the IVIS100 in vivo imaging system

(Caliper). CD-1 female mice were purchased from Charles River. Basal-like mouse mammary gland tumors were obtained from the transgenic mouse mammary tumor model C3-tag (27) (a gift from Mikala Egeblad, Cold Spring Harbor Laboratory, New York). All experiments were performed in agreement with and approved by the Cold Spring Harbor Laboratory Institutional Animal Care and Use Committee.

Two-Photon Microscopy. Mammary glands were harvested and defatted by three rounds of acetone treatment (20 min each). Defatted mammary glands were embedded and imaged according to previously published methods (30). In short, experiments were performed on a high-speed multiphoton microscope with integrated vibratome sectioning (TissueCyte 1000; TissueVision, Inc.). 3D scanning of 5-mm Z-volume stacks was achieved with a microscope objective piezo (PI E-665 LVPZT amplifier and P-725 PIFOC long-travel objective scanner), which translated the microscope objective with respect to the sample. Each optical section was imaged as a mosaic of individual fields of view equal to 0.83 × 0.83 mm and reconstructed posthoc using Fiji and custom-written Matlab software.

Antibodies. Antibodies for flow cytometry were purchased from eBioscience unless otherwise specified, and they include anti-CD24 eFluor® 450, biotinylated and PE-conjugated anti-CD45, biotinylated and phycoerythrin (PE)-conjugated anti-CD31, biotinylated and PE-conjugated anti-Ter119, PE-Cy7-conjugated anti-CD29, FITC- and PE-conjugated anti-CD61, antigen-presenting cell-conjugated anti-CD133, PerCP-Cy5.5- and PE-conjugated anti-Cd1d (clones 1B1 and K253, respectively; BioLegend), PE-conjugated anti-CD22, monoclonal CD59a (Hycult Biotech), PE-conjugated human anti-Cd1d, 7-AAD viability staining solution (BioLegend), FITC-conjugated mouse IgG, and PE-conjugated rabbit IgG. Antibodies for immunostaining were chicken anti-GFP (Invitrogen), mouse monoclonal Cytokeratin 18 (SCTB), anti-chicken-IgG-Alexa Fluor 647 (Invitrogen), and anti-mouse-IgG Alexa Fluor 568 (Invitrogen).

Mammary Gland Preparation. Mammary glands were harvested from young female mice (6–10 wk) and dissociated according to previously published protocol (1). After dissociation, cells were resuspended in 1 mL MACS Buffer (Myltenyi Biotech) and incubated with biotinylated anti-CD45, anti-Ter119, and anti-CD31 antibodies for 20 min. Cells were washed with 10 volumes MACS Buffer and further incubated with antibiotin magnetic microbeads (Myltenyi Biotech). Labeled cells were loaded into a magnetic column attached to a magnetic field (Myltenyi Biotech), and lineage-depleted flow-through cells were collected and further stained.

Flow Cytometry. Cells were stained for 30 min at 4 °C with antibody mix in PBS supplemented with 1% (vol/vol) FBS followed by wash with 10× volume PBS. Cells were resuspended in PBS plus 1% (vol/vol) FBS and further stained with 7-AAD immediately before sorting or analysis. Cells were sorted using a FACS ARII SORP (BD Bioscience). For cell analysis, LRSII (BD Bioscience) cell analyzer or MACSQuant (Myltenyi Biotech) were used. Data analysis was performed using either FloJo (Tree Star) or Diva (BD Bioscience).

Matrigel Colony Assay. Cells were sorted into 96-well plates containing 100 μL chilled 50% (vol/vol) Matrigel Matrix (BD Bioscience), further transferred to 100% Matrigel Precoated Chamber Slides (Lab-Tek), and incubated at 37 °C for 5 min. Complete Growth Media (1) was added to the chamber and renewed every other day for 10 d. Colonies were counted using Nikon Eclipse T1 microscope (Nikon).

Mammary Gland Transplant. Cells were sorted into 96-well plates containing 30 μL 50% (vol/vol) Growth Factor Reduced Matrigel (BD Bioscience) and 0.01% (vol/vol) Tripan Blue (Sigma). Cells were injected into inguinal glands of 3-wk-old females that had been cleared of endogenous epithelium. Recipient glands were removed for evaluation 8–12 wk after cell injection.

Mammary Transplant Analysis. Frozen sections and/or agarose-embedded sections were fixed with 4% paraformaldehyde (Sigma) for 20 min followed by tissue permeabilization and blocking using 10% (vol/vol) goat serum (Sigma). Paraffin-embedded sections were dewaxed and subjected to antigen retrieval for 15 min in Trilogy buffer (Cell Marque) before blocking as described above. Primary antibody staining was performed overnight at 4 °C with constant agitation followed by three washes with 0.1% (vol/vol) Tween 20. Secondary antibody staining was carried out for 45 min at room temperature with constant agitation followed by three washes with 0.1% (vol/vol) Tween 20. Slides were mounted with ProLong Gold supplemented with

DAPI (Invitrogen). For immunohistochemistry detection of GFP-positive outgrowths, the kit Ace IHC Detection Kit (Epitomics) was used according to the manufacturer's instructions. Tissue sections were analyzed using either the Nikon Eclipse T1 microscope (Nikon) or Zeiss LSM 710 confocal microscope. For whole-mount images, glands were harvested, spread atop a glass slide, defatted, and stained with Carmine Aluminum solution prior image analysis. MRU frequency was estimated using the ELDA algorithm (10). Mammary gland reconstitution was considered successful if, by the time of analysis, at least one-third of the fat pad was repopulated with GFP⁺ structures.

RNAseq Library Preparation. Cells were sorted into Eppendorf tubes filled with TRIzol LS (Invitrogen), and RNA purification was performed according to the manufacturer's instructions. DNase-free RNA samples were used for the preparation of double-strand cDNA libraries using the Version 1 Ovation RNAseq System (Nugen). cDNA libraries were phosphorylated, adenylated, and ligated to Illumina adapters followed by PCR enrichment. Single-ended sequencing was performed for 36 cycles in Illumina GAII instruments (Illumina).

RNAseq Mapping and Analysis. We used the Refseq transcriptome (mm9 mouse assembly) downloaded through the University of California, Santa Cruz (USCS) Table Browser (31). Reads were mapped in two stages: first, they were mapped to sequences constructed using all annotated Refseq exons with overlapping exons collapsed, and second, they were mapped to all possible junctions formed from all pairs of exons for the same gene. Mapping was done with RMAP (32) and allowed up to three mismatches in 36 bases. Reads mapping ambiguously (including mapping to an exon and a junction) were discarded. For each Refseq transcript, we counted the number of reads with mapping location that was inside the transcript's exons (allowing a given read to be counted for two distinct transcripts as long as the location is unique) or through one of the transcript's junctions. Reads per kilobase per million (RPKM) calculations discarded duplicate reads and corrected gene size for the portion of the gene that cannot be uniquely mapped. Differential expression between two RNAseq experiments was computed using a 2×2 contingency table and either a χ^2 statistic or Fisher exact test to obtain a *P* value for differential expression. Briefly, the contingency tables contained, for each gene, the counts of reads mapping into the gene and the counts of reads mapping outside the gene for both experiments. The *P* values were corrected for multiple testing using the Bonferroni correction. The genes that remained were called as differentially

expressed (corrected *P* > 0.01), and rankings for differentially expressed genes were based on ratios of RPKM values.

Quantitative PCR. Cells were sorted into 96-well plates containing 30 μ L Cell-To-Ct lysis buffer (Ambion). cDNA synthesis was performed according to the manufacturer's instruction. Real-time PCR was performed using specific Taqman probes (Applied Biosystems) for each gene and *Gapdh* mRNA as an endogenous control. Samples were run on a 7900 Real-Time PCR System (Applied Biosystems).

BrdU Experiment. BrdU label-retaining experiments were performed using the BrdU-APC Flow Kit (BD Bioscience); 3-wk-old female mice were injected with BrdU (one time per day for 5 consecutive d, 50 mg/kg body weight), and mammary glands were harvest at specified time points. Mammary gland cells were prepared according to the BrdU manufacturer's recommendations. Cells were analyzed with an LSRII Cell Analyzer (BD Bioscience), and 1 million cells were recorded per sample. For each experiment (*n* = 2), three glands were analyzed at week 0 (last day of BrdU injection), and three glands were analyzed at week 12 after BrdU injection.

Knockdown Experiment. shRNAs against 56 selected genes were pulled and transferred from pGIPz (LMN vector) lentiviral backbone (Open Biosystems) to MSCV-miR30-PGK-NEO-IRES-GFP retroviral backbone (a gift from Christopher R. Vakoc, Cold Spring Harbor Laboratory, New York). Plasmid was transfected into Plat-E cells (33) using Lipofectamine 2000 and vesicular stomatitis virus g-protein (VSVG), and virus was collected 24 and 36 h posttransfection. Cells were infected by spin infection and allowed 2 d for recovery. GFP levels were measured using MACSQuant Cell analyzer (Miltenyi Biotec) from 10,000 cells. Hairpins used on validation experiments were ordered as oligonucleotides from Integrated DNA Technologies (IDT) and used as the template for PCR reactions using KOD hot-start polymerase (EMD Millipore) and the primers 5MIR (5'-CAGAAGGCTCGAGAAGGTATATGCTGTGACAGTGAGCG-3') and 3MIR (5'-CTAAGTAGCCCTTGAATTCGAGGAGTAGGCA-3'). PCR products were column-purified (Qiagen), digested with EcoRI and XhoI enzymes, and cloned into predigested LMN vectors using T4 rapid ligase (Promega).

ACKNOWLEDGMENTS. We thank Elaine Fuchs, Mikala Egeblad, and Christopher R. Vakoc for valuable mouse stains and reagents. This work was supported by National Institutes of Health Grand Opportunity Award #1 RC2 CA148507 and P01 Award 2P01CA013106.

- Shackleton M, et al. (2006) Generation of a functional mammary gland from a single stem cell. *Nature* 439(7072):84–88.
- Stingl J, et al. (2006) Purification and unique properties of mammary epithelial stem cells. *Nature* 439(7079):993–997.
- Bai L, Rohrschneider LR (2010) s-SHIP promoter expression marks activated stem cells in developing mouse mammary tissue. *Genes Dev* 24(17):1882–1892.
- Tu Z, et al. (2001) Embryonic and hematopoietic stem cells express a novel 5H2-containing inositol 5'-phosphatase isoform that partners with the Grb2 adapter protein. *Blood* 98(7):2028–2038.
- Visvader JE, Lindeman GJ (2006) Mammary stem cells and mammapoiesis. *Cancer Res* 66(20):9798–9801.
- Tumbar T, et al. (2004) Defining the epithelial stem cell niche in skin. *Science* 303(5656):359–363.
- Mikaelian I, et al. (2006) Expression of terminal differentiation proteins defines stages of mouse mammary gland development. *Vet Pathol* 43(1):36–49.
- Smalley M, Ashworth A (2003) Stem cells and breast cancer: A field in transit. *Nat Rev Cancer* 3(11):832–844.
- Neville MC (2009) Introduction: Transplantation of the normal mammary gland: Early evidence for a mammary stem cell. *J Mammary Gland Biol Neoplasia* 14(3):353–354.
- Hu Y, Smyth GK (2009) ELDA: Extreme limiting dilution analysis for comparing depleted and enriched populations in stem cell and other assays. *J Immunol Methods* 347(1–2):70–78.
- Asselin-Labat ML, et al. (2008) Delineating the epithelial hierarchy in the mouse mammary gland. *Cold Spring Harb Symp Quant Biol* 73:469–478.
- Molofsky AV, Pardo R, Morrison SJ (2004) Diverse mechanisms regulate stem cell self-renewal. *Curr Opin Cell Biol* 16(6):700–707.
- Adams EJ, López-Sagasetta J (2011) The immutable recognition of CD1d. *Immunity* 34(3):281–283.
- Qin X, et al. (2001) Genomic structure, functional comparison, and tissue distribution of mouse Cd59a and Cd59b. *Mamm Genome* 12(8):582–589.
- Haas KM, et al. (2006) CD22 ligand binding regulates normal and malignant B lymphocyte survival in vivo. *J Immunol* 177(5):3063–3073.
- Greenlee MC, Sullivan SA, Bohlsos SS (2008) CD93 and related family members: Their role in innate immunity. *Curr Drug Targets* 9(2):130–138.
- Becker-Herman S, Arie G, Medvedovsky H, Kerem A, Shachar I (2005) CD74 is a member of the regulated intramembrane proteolysis-processed protein family. *Mol Biol Cell* 16(11):5061–5069.
- Medina D, Oborn CJ, Kittrell FS, Ullrich RL (1986) Properties of mouse mammary epithelial cell lines characterized by in vivo transplantation and in vitro immunocytochemical methods. *J Natl Cancer Inst* 76(6):1143–1156.
- Danielson KG, et al. (1989) Clonal populations of the mouse mammary cell line, COMMA-D, which retain capability of morphogenesis in vivo. *In Vitro Cell Dev Biol* 25(6):535–543.
- Deugnier MA, et al. (2006) Isolation of mouse mammary epithelial progenitor cells with basal characteristics from the Comma-Dbeta cell line. *Dev Biol* 293(2):414–425.
- Ibarra I, Erlich Y, Muthuswamy SK, Sachidanandam R, Hannon GJ (2007) A role for microRNAs in maintenance of mouse mammary epithelial progenitor cells. *Genes Dev* 21(24):3238–3243.
- Chan CW, et al. (2007) A novel member of the SAF (scaffold attachment factor)-box protein family inhibits gene expression and induces apoptosis. *Biochem J* 407(3):355–362.
- Van Keymeulen A, et al. (2011) Distinct stem cells contribute to mammary gland development and maintenance. *Nature* 479(7372):189–193.
- Lim E, et al. (2010) Transcriptome analyses of mouse and human mammary cell subpopulations reveal multiple conserved genes and pathways. *Breast Cancer Res* 12(2):R21.
- Dexter DL, et al. (1978) Heterogeneity of tumor cells from a single mouse mammary tumor. *Cancer Res* 38(10):3174–3181.
- Teng MW, et al. (2007) Combined natural killer T-cell based immunotherapy eradicates established tumors in mice. *Cancer Res* 67(15):7495–7504.
- Green JE, et al. (2000) The C3(1)SV40 T-antigen transgenic mouse model of mammary cancer: Ductal epithelial cell targeting with multistage progression to carcinoma. *Oncogene* 19(8):1020–1027.
- Hix LM, et al. (2011) CD1d-expressing breast cancer cells modulate NKT cell-mediated antitumor immunity in a murine model of breast cancer metastasis. *PLoS One* 6(6):e20702.
- Spanoudakis E, et al. (2009) Regulation of multiple myeloma survival and progression by CD1d. *Blood* 113(11):2498–2507.
- Ragan T, et al. (2012) Serial two-photon tomography for automated ex vivo mouse brain imaging. *Nat Methods* 9(3):255–258.
- Karolchik D, et al. (2004) The UCSC Table Browser data retrieval tool. *Nucleic Acids Res* 32(Database issue):D493–D496.
- Smith AD, et al. (2009) Updates to the RMAP short-read mapping software. *Bioinformatics* 25(21):2841–2842.
- Morita S, Kojima T, Kitamura T (2000) Plat-E: An efficient and stable system for transient packaging of retroviruses. *Gene Ther* 7(12):1063–1066.

Supporting Information

dos Santos et al. 10.1073/pnas.1303919110

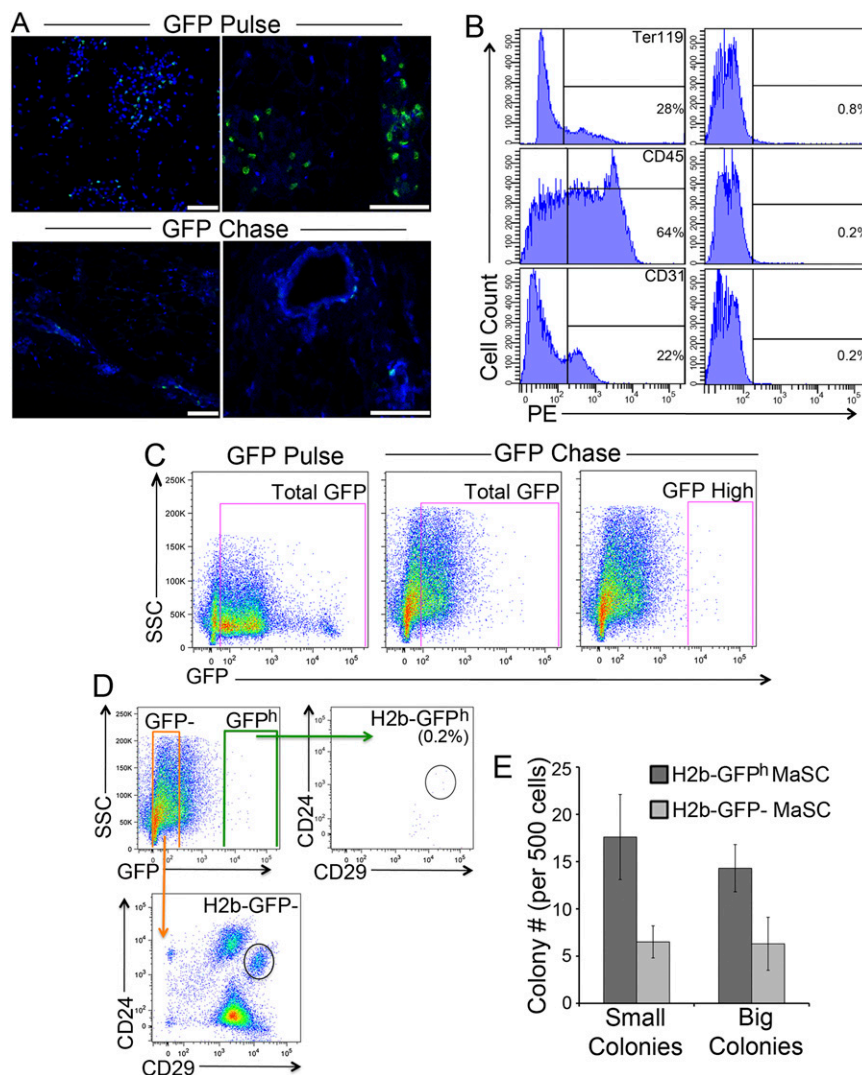


Fig. S1. Characterization of H2b-GFP mammary gland label-retaining cells. Effects of doxycycline diet on K5tTa-H2b-GFP transgenic mouse mammary glands. (A) Paraffin-embedded sections with DAPI nuclear staining and anti-GFP antibody. (B) Lineage depletion strategy. FACS analysis showing removal of PE-stained red blood cells (Ter119⁺ cells), white blood cells (CD45⁺ cells), and endothelial cells (CD31⁺ cells) after magnetic bead lineage depletion. (C) H2b-GFP⁺ cells gating strategy. Lin⁻ mammary gland cells were first selected according to GFP expression (GFP⁻ and GFP⁺) and further analyzed according to anti-CD24 and anti-CD29 staining as displayed in Fig. 2. (D) FACS sorting strategy for transplantation assays. Lin⁻ GFP chase cells, stained with 7-ADD for dead cell exclusion, were divided based on GFP expression, H2b-GFP⁻ mammary gland stem cells (MaSCs; CD24⁺CD29^hGFP⁻), and H2b-GFP^h MaSCs (CD24⁺CD29^hGFP^h) and either transplanted into cleared fat pads of prepubescent female mice or (E) carried through to colony-forming assays.

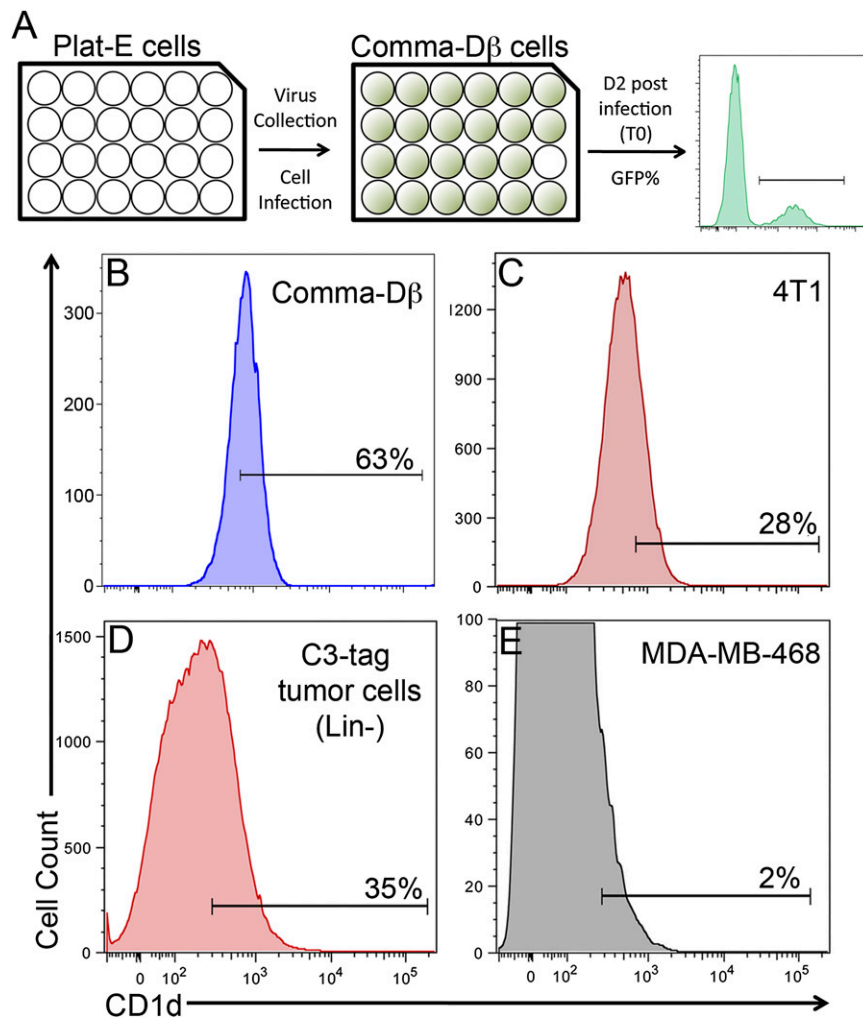


Fig. S4. Mammary gland-focused screen. (A) Screen strategy scheme. Plat-E cells were transfected with shRNAs as described in *Materials and Methods*. Comma-D β cells were infected with the virus supernatant for 20 h; 48 h postinfection, GFP percent was quantified using the MACSQuant Cell Analyzer (Miltenyi Biotech). T0 represents the GFP percent on day 2 postinfection, and T3 represents the GFP percent on day 12 d postinfection. CD1d⁺ cells in mouse cell lines (B) Comma-D β cells, (C) 4T1 mouse breast cancer cells, and (D) C3-tag breast cancer model primary cells. (E) CD1d⁺ in the human cell line MDA-MB-468.

Dataset S1. Mammary reconstitution unit (MRU) frequency in H2b-GFP^h MaSC

[Dataset S1](#)

Reconstituted mammary glands harvested 12 wk postinjection of either H2b-GFP^h MaSCs or H2b-GFP⁻ MaSCs. A minimum of 25 outgrowths is required to be considered a reconstituted gland. MRU frequency was estimated using the ELDA algorithm.

Dataset S2. Mammary gland pathway analysis

[Dataset S2](#)

Top differentially expressed genes of all mammary gland cell types were analyzed for pathway enrichment and molecular functions using Ingenuity Pathways Analysis (Ingenuity Systems). A minimum of 50 genes per cell type was analyzed.

Dataset S3. MRU frequency in CD1d+ MaSC[Dataset S3](#)

Total MaSC cells (CD24⁺CD29^h) and CD1d MaSC cells (CD24⁺CD29^hCD1d⁺) were isolated from the H2b-GFP transgenic mouse off doxycycline diet (GFP pulse). Reconstituted mammary glands harvested 12 wk postcell injection. A minimum of 25 outgrowths is required to be considered a reconstituted gland. MRU frequency was estimated using the ELDA algorithm.